sciendo

Theoretical modeling of optical spectra of N(1) and N(10) substituted lumichrome derivatives

Denisa Cagardová[1], Jan Truksa[2], Martin Michalík[1], Jan Richtár[2], Jozef Krajčovič[2], Martin Weiter[2], Vladimír Lukeš[1]

[1]Institute of Physical Chemistry and Chemical Physics, Slovak University of Technology in Bratislava, Radlinského 9, SK-812 37 Bratislava, Slovakia
[2]Faculty of Chemistry, Brno University of Technology, Purkyňova 118, CZ-612 00 Brno, Czech Republic
denisa.cagardova@stuba.sk

Abstract: A systematic study of (7,8-dimethylated) alloxazine, isoalloxazine, and their derivatives with substituted N(1) and N(10) positions was conducted using the density functional theory. The main aim of this work was the direct investigation of substituent effect on the molecular structure. Furthermore, HOMED aromaticity indices were calculated to describe the scope of the geometry changes. Frontier molecular orbitals of reference alloxazine, isoalloxazine and lumichrome derivatives were discussed by means of changes in their shape and energy levels. Photophysical properties were analyzed by determination of optical transition energies using the TD-DFT method. Obtained results were compared with previously published experimental data.

Keywords: Aromaticity index; vertical excited transitions; excited states; fluorescence; lumichrome; alloxazine

Introduction

Photochemical and photophysical properties of alloxazine and its derivatives have been studied since 1966 (Kozioł, 1966). Methyl-substituted alloxazines, mainly riboflavin and lumichrome are present in many foods and they play a key role in many enzymatic reactions and processes such as phototropism and phototaxis (Ai et al., 2010). Although the parent alloxazine and isoalloxazine are closely related compounds (see Fig. 1), the shift of a hydrogen atom from position N(1) to N(10) causes

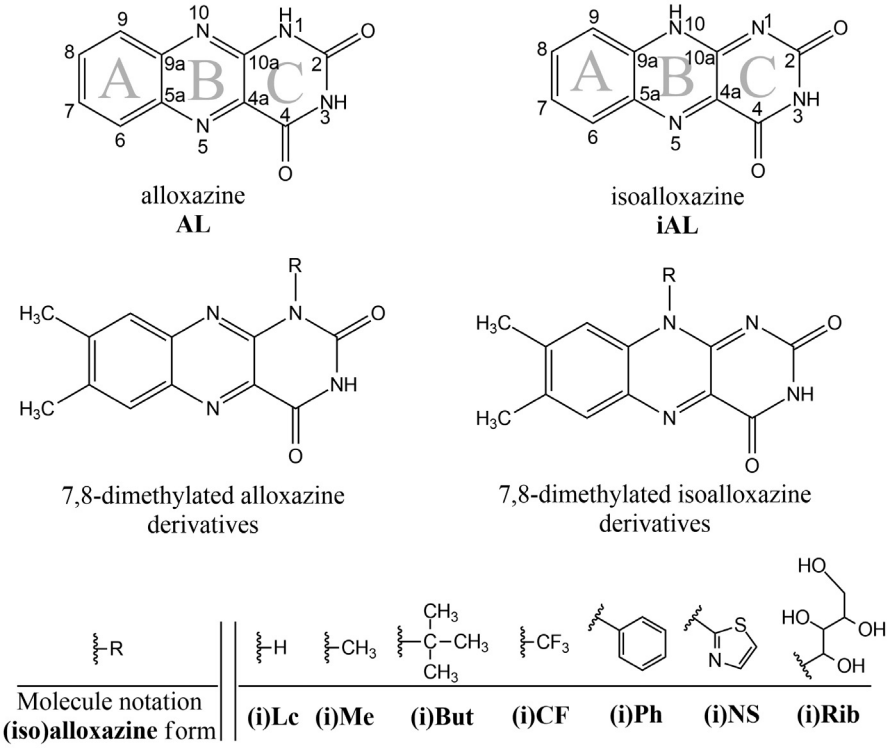

Fig. 1. Schematic structure of studied molecules: ring and atom notation of the benzo[g]pteridine moiety applied for all derivatives.

significant changes in their spectroscopic and photophysical properties.

Alloxazine exhibits absorption spectra differing from those of isoalloxazine by a hypsochromic shift of both long-wavelength maxima from about 440 nm and 340 nm to about 380 nm and 330 nm (Sikorska et al., 2004a). Moreover, isoalloxazine exhibits one order of magnitude larger fluorescence quantum yields and correspondingly longer fluorescence lifetimes than alloxazine. At pH = 10, the presence of isoalloxazine (9 %) is expected while at pH = 4, the solution does not contain the tautomeric isoalloxazine form (Penzkofer, 2016). The fluorescence wavelength maximum of an alloxazine sample in an aqueous solution at pH = 4 for fluorescence excitation wavelength λ_{exc} = 330 nm is 456 nm. At pH = 10, the emission wavelength of 530 nm is observed for the fluorescence excitation wavelength λ_{exc} = 440 nm. The first absorption bands of alloxazine and lumichrome show minimal environmental dependence. A significant effect of polarity and proticity of the solvent was observed for their second absorption band (Salzmann and Marian, 2009). Surprising differences between these two molecules were found in the absorption strength, fluorescence lifetime, fluorescence quantum yield, and thermal ground-state tautomeric content at pH = 10. The absorption spectrum of riboflavin and iso-(6,7)-riboflavin in methanol shows two characteristic bands at longer wavelengths, with the maxima at approximately 360 nm and 444 nm for riboflavin; and at 343 nm and 447 nm for iso-(6,7)-riboflavin, which indicates the effect of the methyl group position on the shorter-wavelength maximum. The effect of methyl group on the positions of absorption maxima was examined by Sikorska et al. using both experiment and theory with a broad range of (iso)alloxazine derivatives (Sikorska et al., 2004b; Sikorska et al., 2004c).

Available information about the chemical and electronic structure of (iso)7,8-dimethyl-alloxazine substituted in position N(1) or N(10) is incomplete. Previous experimental and theoretical studies of these compounds were focused on two substituents — methyl and 2,3,4,5-tetrahydroxypentyl groups (Gross et al., 1996; Sikorska et al., 2005; Zanetti-Polzi et al., 2017). Therefore, theoretical analysis of 14 derivatives based on the modification of the initial benzo[g]pteridine moiety in (iso) alloxazine by 7,8-dimethylation and substitution in N(1) or N(10) positions (Fig. 1) is presented here. In laboratory practice, the selected functional groups can be synthetically added to the benzo[g]pteridine moiety into selected positions. Partial aims of this study are: (1) to calculate optimal geometries of the electroneutral molecules and selected lowest energy excited electronic states; (2) to evaluate the energies of frontier molecular orbitals (MOs) and (3) to calculate optical transitions contributing to the lowest energy in absorption and fluorescence spectra.

Computational details

The Gaussian 09 program package (Frisch et al., 2013) was applied for all quantum chemical calculations by means of the density functional theory. In these calculations, the B3LYP hybrid functional (Lee et al., 1988; Becke, 1988) without any constraints (energy cut-off of 10^{-5} kJ · mol^{-1}, final RMS energy gradient under 0.01 kJ · mol^{-1} · A^{-1}) was used. A sufficiently large basis set of atomic orbitals 6-311++G** was applied (Hariharan and Pople, 1973; Rassolov et al., 1998). In search of optimized B3LYP geometries, the time dependent TD-DFT method was used. As a result, vertical singlet and triplet transition energies and the corresponding oscillator strengths between the initial and final electronic states were determined (Furche and Ahlrichs, 2002). The molecules and their frontier molecular orbitals were visualized using the Molekel (Flukiger et al., 2002) and Avogadro (Hanwell et al., 2012) program packages.

Aromaticity of molecules gives significant information about their chemical structure. One way to describe aromaticity is the structure-based Harmonic Oscillator Model of Electron Delocalization (HOMED) index (Cyrañski et al., 2002; Frizzo and Martins, 2012), which describes the bond length changes in molecules of interest with respect to the reference aromatic molecules. The index can be calculated by the equation:

$$\mathrm{HOMED} = 1 - \frac{1}{m}\left\{\alpha_{XY}\sum_{i=1}^{m}\left(R(XY)_{ref} - R(XY)_i\right)^2\right\} \qquad (1)$$

where m stands for the number of bonds considered in the investigated aromatic ring, $R(XY)_{ref}$ is the reference bond length, α_{XY} is a normalization constant (see below) and $R(XY)_i$ is the actual bond length between X and Y atoms.

In case of the studied derivatives, C—C, C—N and C—N(H) aromatic bond lengths were determined. Suitable reference quantities, R_{ref}, used in Eq(1) were obtained from the B3LYP/6-311++G** optimized structures of benzene, 1,3,5-triazine and pyrrole molecules for CC, CN and CN(H) bonds, respectively. The proposed R_{ref} values for the basis set are: 1.3943 Å ($R(CC)_{ref}$), 1.3344 Å ($R(CN)_{ref}$) and 1.3749 Å ($R(CN(H))_{ref}$). Normalization constants α_{XY} were calculated as follows (Ośmiałowski et al., 2006):

$$\alpha(XY) = \qquad (2)$$
$$= 2\left\{\left(R(XY)_{ref} - R(XY)_{sin}\right)^2 + \left(R(XY)_{ref} - R(XY)_{doub}\right)^2\right\}^{-1}$$

where the reference single R_{sin} and double R_{doub} bond lengths were taken from the optimized structures of ethane and ethene (CC bonds), N—$(CH_3)_3$ and H_2C=N—CH_3 (CN bonds), $(H_3C)_2$—NH and H_2C=NH (CN(H) bonds) molecules, respectively (Allen et al., 1987). The calculated B3LYP R_{sin} bond lengths are: 1.5317 Å (C—C), 1.4554 Å (C—N) and 1.4574 Å for the C—N(H) bond. Moreover, the double bond lengths R_{doub} of 1.3289 Å (C=C), 1.2631 Å (C=N) and 1.2672 Å (C=N(H)) were used to determine α_{XY} from Eq(2). The corresponding normalization constants are: α(CC) = 86.40 Å^{-2}, α(CN) = 101.41 Å^{-2} and α(CN(H)) = 108.66 Å^{-2}. The maximal HOMED value of one was assigned to the benzene molecule by convention.

Results and Discussion

Although isobutyl, methyl, trifluoromethyl, thiazole, and 2,3,4,5-tetrahydroxypenthyl substituents show many conformations, chemical structure of the benzo[g]pteridine core is not affected significantly. As seen in Tab. 1, HOMED(A) indices of the isoalloxazine form are consistently by ca. 0.04 higher than those of the alloxazine counterparts. Moreover, dimethylation in C(7) and C(8) positions causes a decrease in the A ring aromaticity (see **Lc**/**iLc**), while additional substitutions slightly increase the HOMED(A).

With respect to the parent **AL** and **iAL** molecules, the HOMED(C) index is much lower for the isoalloxazine derivatives than for the alloxazine forms, with exception of (**i**)**NS**, (**i**)**CF** and (**i**)**But** tautomer couples. This effect is the most significant for **CF** and **But**, possibly because CF_3 is a strongly electron-withdrawing group and tert-butyl group is relatively bulky and electron-donating group with much higher positive inductive effect than the methyl group in **Me**. They cause the most significant decrease in the aromaticity possibly because of the distortion due to steric repulsion and strong inductive effect. **NS** contains larger atoms than carbon, so some steric distortion is expected, but it is smaller due to the two-dimensional nature of the ring. Moreover, in case of substituted rings, the comparison is complicated by the fact that the substituents in tautomers are present on different rings. Therefore, it makes more sense to compare the substitution effect of the C ring in the alloxazine form to the B ring in isoalloxazine form and vice versa (see Fig. 1). Two methyl groups attached to the A ring in **Lc** and **iLc** cause an increase of HOMED for both B and C rings. Additional substitution to the B (C) ring of **iLc** (**Lc**) significantly decreases the aromaticity of the substituted ring. Relative changes correspond to the differences between HOMED of the studied molecule and the reference alloxazine/isoalloxazine molecule divided by the HOMED of reference. Relevant changes of HOMED indices in comparison to alloxazine and isoalloxazine molecules are shown in Fig. 2. Note that all studied derivatives, apart from two methyl groups at C(7) and C(8) atoms such as lumichrome **Lc,** have also another additional substituent. Thus, the B and/or C ring substitution effect is cumulative with respect to the two methyl groups. These side methyl groups bonded to the A ring increase the aromaticity by up to 2 % for both (un)substituted rings in tautomers.

In case of the HOMED index of substituted rings, i.e. C ring of alloxazine derivative and B ring of iso-form, all studied additional substituents decrease their aromaticity (see Tab. 1 and Fig. 2a). The bond length changes caused by the presence of a double bond in the C ring of the iso-form also affect HOMED(C), which is more likely to be visible in molecules with smaller or linear substituents. A similar case may be argued for the HOMED(B) index of isoalloxazine derivatives where the ring lacks a double bond and is influenced by the substituent which leads to a significant distortion of geometry. The largest decrease of around 30 % has been found for the **CF**/**iCF** derivatives while butyl group brings the HOMED indices down by 18 %. It occurs mainly by exceptional ring distortion due to CF_3 because of the above-mentioned strong electron-withdrawing

Tab. 1. HOMED indices of A, B and C rings of studied molecules.

Molecule	A	B	C	Molecule	A	B	C
AL	0.942	0.924	0.814	**iAL**	0.983	0.867	0.664
Lc	0.930	0.934	0.821	**iLc**	0.975	0.880	0.678
Me	0.934	0.933	0.724	**iMe**	0.975	0.798	0.690
But	0.938	0.928	0.668	**iBut**	0.975	0.735	0.680
CF	0.932	0.938	0.585	**iCF**	0.982	0.668	0.645
Ph	0.933	0.934	0.696	**iPh**	0.975	0.784	0.683
NS	0.932	0.935	0.671	**iNS**	0.977	0.763	0.677
Rib	0.936	0.933	0.723	**iRib**	0.974	0.794	0.695

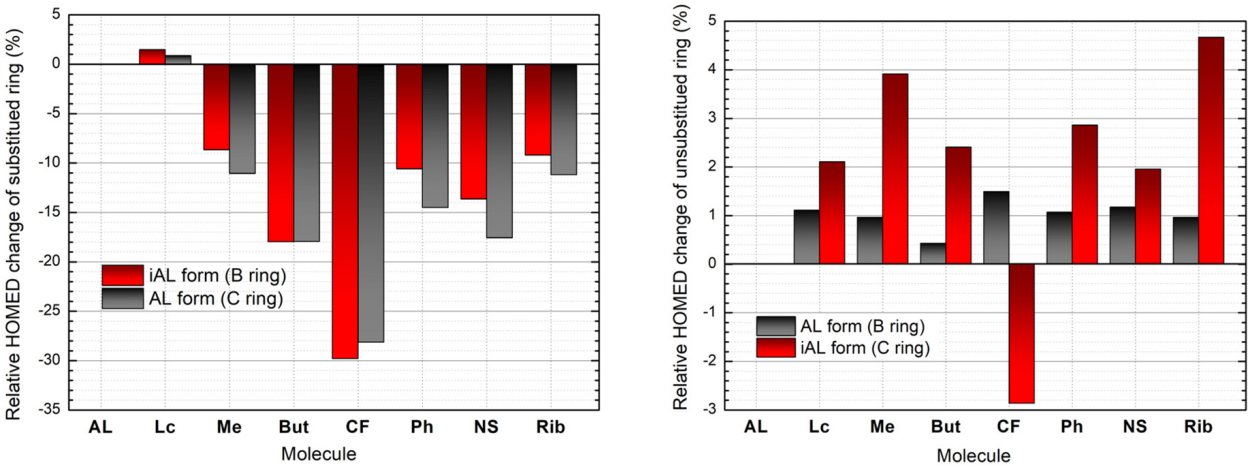

Fig. 2. Relative changes of HOMED indices of a) substituted C/B ring and b) unsubstituted B/C ring of alloxazine/isoalloxazine derivatives.

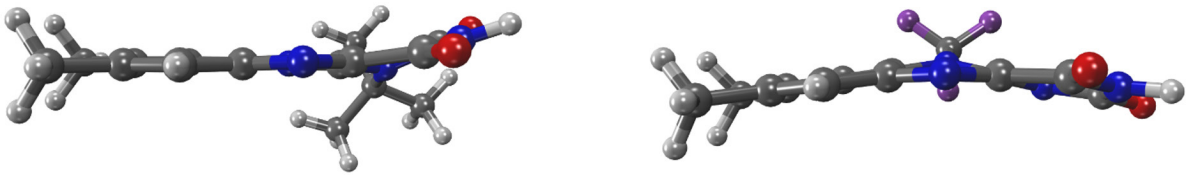

But iCF

Fig. 3. Distortion of rings observable in optimal geometry of **But** and **iCF**.

effect of the group and bulky tert-butyl substituent (e.g. see **But** and **iCF** ring distortion in Fig. 3).

Based on Fig. 2a, the smallest changes of aromaticity in the substituted rings in comparison to their parent (iso)alloxazine molecules are caused by the methyl group in **(i)Me**. Large 2,3,4,5-tetrahydroxypentyl substituent in **(i)Rib** had minimal influence on the HOMED indices. These comparatively small relative changes in HOMED indicate less significant substituent influence (up to 12 %) than the remaining additional substituents, which supports the above-mentioned steric effect hypothesis and small inductive effect.

In heterocyclic rings without a substituent (see Fig. 2b), i.e. B ring of alloxazine and C ring of isoalloxazine, small substituent-induced HOMED increase of up to 5 %, with exception for **iCF,** can be seen. Interestingly, isoalloxazine forms are much more affected; however, it is still considered to be negligible in comparison to HOMED changes of substituted ring. Based on these results, the **iCF** derivative is the least stable within the studied group as the trifluoromethyl group consistently decreases the aromaticity, as evaluated by HOMED indices.

Energy levels of frontier molecular orbitals and their shape allow estimating the electronic structure. Fig. 4 shows energy levels of the highest occupied (HOMOs) and lowest unoccupied (LUMOs) molecular orbitals. The B3LYP HOMO and LUMO energies for alloxazine **AL**/isoalloxazine **iAL** are: –7.18 eV/–7.04 eV and –3.17 eV/–3.53 eV, respectively. In case of two methyl groups addition to C(7) and C(8) in **Lc/iLc**, a slight increase of both HOMO (–6.91 eV/–6.76 eV) and LUMO (–2.97 eV/–3.34 eV) energies can be seen, so the constriction of energy gap occurs. The substitution group variation alters the orbital energies in different ways.

Methyl (**Me/iMe**), butyl (**But/iBut**), phenyl (**Ph/iPh**), and 2,3,4,5-tetrahydroxypentyl (**Rib/iRib**) functional groups have comparable influence on the energies of frontier MOs. Differences are found only between the alloxazine and isoalloxazine forms. Isoalloxazine forms generally have smaller HOMO to LUMO energy difference. Minimal LUMO energy of –3.66 eV was found for the **iCF** derivative. The highest B3LYP HOMO energy is predicted for **iRib** (–6.33 eV) while the **CF** molecule exhibited the lowest one of –7.23 eV.

As it is depicted in Fig. 5, frontier MOs are delocalized over the whole molecule in all cases indicating an effective π-conjugation in the central fused systems. HOMO and LUMO orbitals of the studied molecules have a π-electron character, but the electron clouds are not as uniformly delocalized as in the parent alloxazine and isoalloxa-

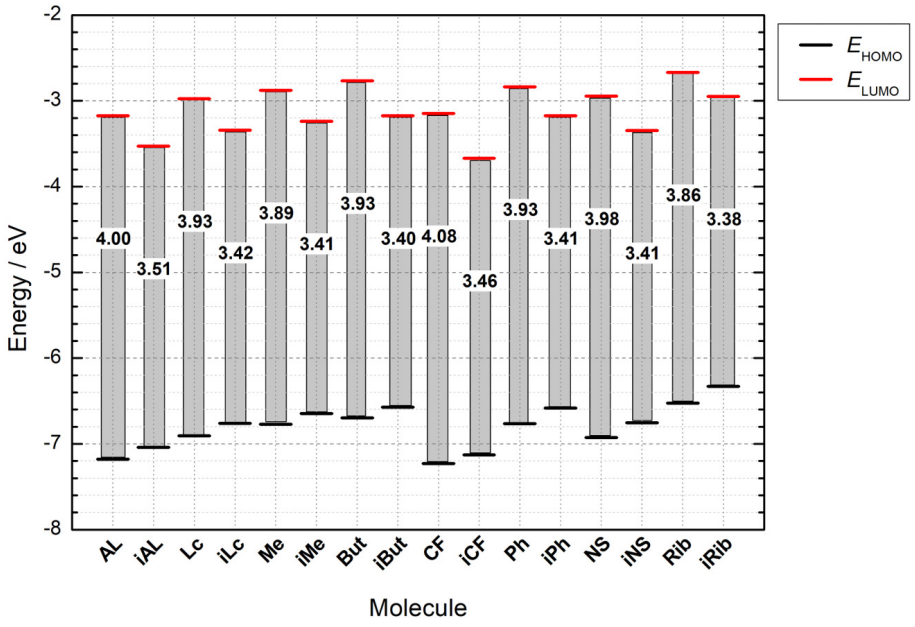

Fig. 4. Energy diagram of B3LYP frontier molecular orbitals for the neutral state of studied molecules. Energy differences between the frontier molecular orbital levels are depicted by grey rectangles and the value corresponds to the energy gap in eV.

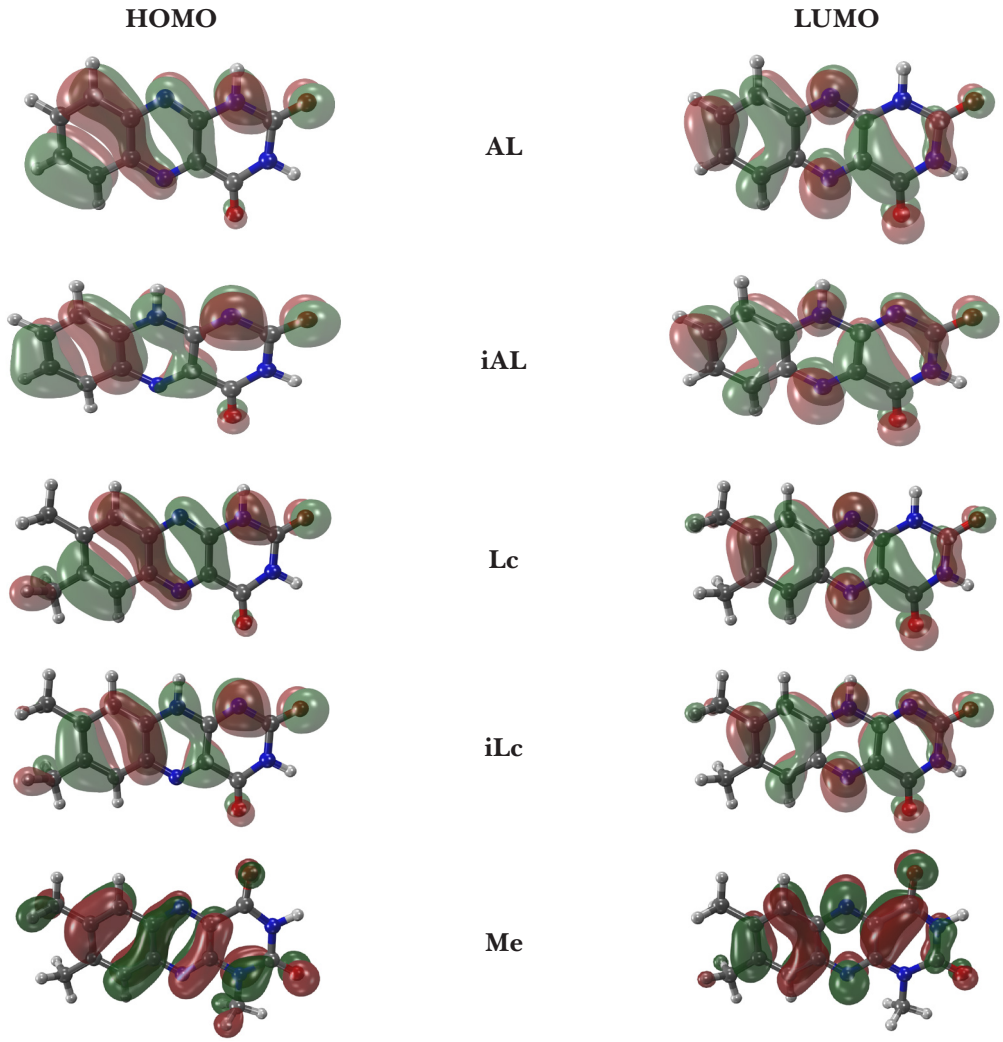

Fig. 5. Shapes of frontier molecular orbitals of studied molecules. Iso-surface value is 0.025.

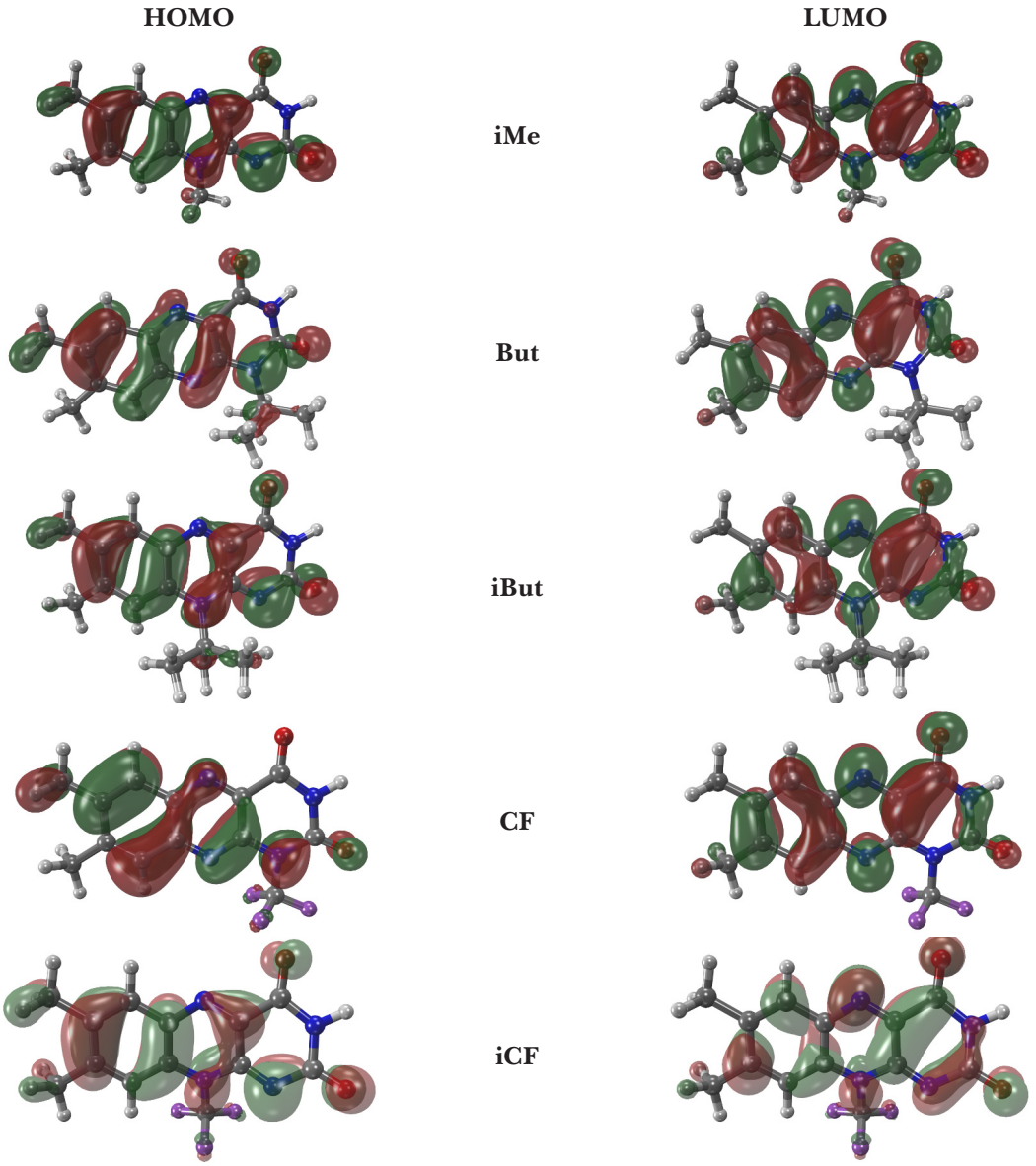

Fig. 5. (continued) Shapes of frontier molecular orbitals of studied molecules. Iso-surface value is 0.025.

zine molecules. Shapes of the orbitals are modulated by the bonding of methyl groups in C(7) and C(8) positions and by the additional studied substitution. Nevertheless, for all studied molecules, the lobes of HOMOs are absent over the C(2) atom and they are present over the methyl group in the vicinity of the C(7) atom. Interestingly, very small electronic clouds were found over the fluorine atoms in (**i**)**CF** and hydrogen atoms in additional methyl group in (**i**)**Me** derivatives. The electron withdrawing CF_3 group also causes an electron cloud formation over the hydrogens of the CH_3-C(7) group and another cloud above CH_3-C(8) occurs in its iso-tautomer. In case of LUMO lobes, distribution of isoalloxazine derivatives, clouds are mostly delocalized over the whole benzo[g]pteridine moiety. On the other hand, molecules in the alloxazine form show lower delocalization over the N(1) nitrogen which is attached to the substituted functional group.

Parent (iso)alloxazine molecules and their alkyl substituted derivatives exhibit experimental absorption spectra with several major bands in the ultraviolet-visible region. For example, the first experimental band maxima of **AL** (Sikorska et al., 2004a) and **Lc** (Sikorski et al., 1998) in aqueous solution are found at 3.27 eV (379 nm) and 3.22 eV (385 nm), respectively. The second absorption band is located at 3.87 eV (320 nm) for alloxazine and at 3.71 eV (334 nm) for lumichrome (**Lc**). Comparison of the lowest vertical gas-phase TD-B3LYP energies for the singlet states is provided in Fig. 6. For alloxazine, energy of the first excited vertical singlet state (S_1) over the electronic ground state is 3.38 eV (367 nm). The corresponding oscillator strength is negligible. This forbidden excitation comes from

an n-type molecular orbital to π*-type HOMO–2 to LUMO transition. The second excited singlet state, related to the HOMO to LUMO transition, is merely 0.06 eV above the S_1 state with $^1(\pi\pi^*)$ character. According to the previously published results, the third excited singlet state (S_3) has $^1(n\pi^*)$ character. The vertical excitation energy of this $S_0 \rightarrow S_3$ transition is 3.93 eV (315 nm) and the oscillator strength is negligible. The fourth vertical optical transition has a significant oscillator strength of 0.16 and the corresponding excitation energy is 3.97 eV (313 nm). For lumichrome **Lc**, first absorption band occurs at 3.39 eV (366 nm), which is insignificantly shifted compared to alloxazine **AL**, thus the two methyl groups bonded to the A ring have negligible effect on the absorption band maxima. Interestingly, oscillator strength increases to 0.06 and this first absorption band matches the HOMO→LUMO transition. The same situation can be observed in iso-tautomers **iAL** and **iLc**. $S_0 \rightarrow S_1$ energies of 3.09 eV (400 nm) with $^1(n\pi^*)$ character for **iAL** and 3.02 eV (411 nm) with $^1(\pi\pi^*)$ character for **iLc** show that dimethylation to C(7) and C(8) slightly decreases the transition energy. However, HOMO→LUMO transition occurs in **Lc** with the corresponding oscillator strength of 0.20, while in **iAL,** HOMO–1 to LUMO transition occurs with negligible oscillator strength. The second excitation of **iAL** (transition from HOMO to LUMO) exhibits the $^1(\pi\pi^*)$ character with oscillator strength of 0.17. Changes in electron distribution and aromaticity of the iso-form within tautomer couples lead to the bathochromic shifts of the lowest energy transitions compared to the alloxazine forms. In case of additional substitution of methyl to the B or C ring for (**i**)**Me**, the calculated TD-B3LYP excitation energies are red shifted in comparison to (**i**)**Lc**, i.e. 3.37 eV (368 nm), 3.40 eV (364 nm) for the first two excitation energies for **Me**. Slightly higher vertical excitation energies (3.41 eV, 3.47 eV, 3.86 eV, 4.02 eV for **AL** and 3.44 eV, 3.41 eV, 3.89 eV, 3.91 eV for **Me**) were obtained using a combination of the density functional and multi-reference configuration interaction method (DFT/MRCI) (Grimme and Waletzke, 1999).

TD-B3LYP predicts zero oscillator strengths for vertical triplet excitations. For **AL**, **Lc** and their substituted derivatives, the lowest energy triplet excitation $S_0 \rightarrow T_1$ ranges between 2.50 eV and 2.65 eV while the iso-forms of tautomer couples show the energy slightly above 2 eV. According to the previously published works (Sikorska et al., 2004d), the $S_0 \rightarrow T_1$ transition has $^3(\pi\pi^*)$ character.

Experimental fluorescence emission spectra of the studied molecules show a single band where the exact position of the maximum depends on the environment and tautomeric forms. For example, maxima of the fluorescence emission measured in acetonitrile are 2.79 eV (444 nm) for alloxazine (**AL**) and 2.84 eV (436 nm) for lumichrome (**Lc**). The fluorescence emission spectrum of lumiflavin (**iMe**) and riboflavin (**iRib**) in methanol (Sikorska et al., 2005) show a band with the maxima at 2.37 eV (526 nm) and 2.33 eV (532 nm), respectively. Isoalloxazine exhibits one order of magnitude higher fluorescence quantum yields and cor-

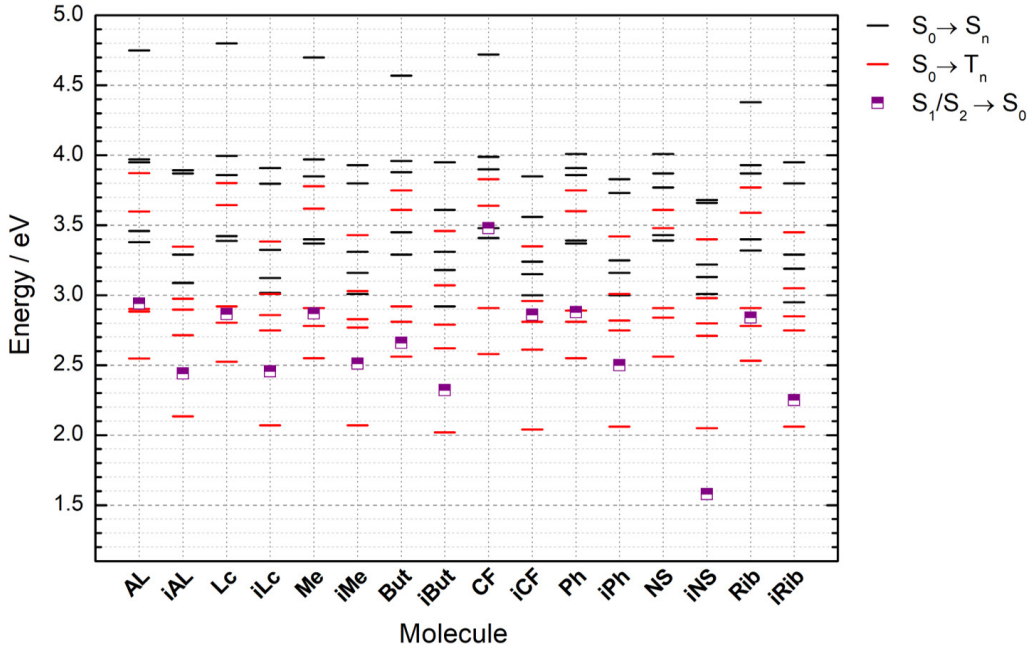

Fig. 6. Energy diagram of selected lowest energy vertical TD-B3LYP singlet ($S_0 \rightarrow S_n$) and triplet ($S_0 \rightarrow T_n$) excitation energies for optimal electronic-ground state geometries and $S_1/S_2 \rightarrow S_0$ deexcitation energies.

respondingly longer fluorescence lifetimes than alloxazine. At the level of time dependent DFT, many optimal geometries of the excited singlet and triplet states of alloxazine derivatives represent a saddle point. As it was reported by Salzmann et al. (2009), one imaginary frequency is obtained for out-of-plane deformation. Nevertheless, TD-DFT deexcitation energies agree with the DFT/MRCI results for the alloxazine and isoalloxazine derivatives.

As it was proved by Sikorska et. al. (2005) for riboflavin (**iRib**), the $^1(\pi\pi^*)$ to $^3(\pi\pi^*)$ intersystem crossing increases the quantum yield of triplet oxygen formation and decreases the quantum yields of singlet oxygen formation with a suitable energy levels difference to influence the $^1O_2$ to $^3O_2$ conversion (Min and Boff, 2006). Since riboflavin (**iRib**) is already in use as a photo-antimicrobial agent with the excitation wavelength of 450 nm (Min and Boff, 2006), a derivative with similar singlet and triplet energy levels has possible future application in medicine. Our theoretical calculations show that the singlet to triplet energy difference of the HOMO→LUMO transition is clearly modulated by tautomerization.

Conclusions

Optimal geometries and electronic structure of (iso)alloxazine, lumichrome, and its model substituted tautomeric derivatives were investigated using the density functional theory. Changes in molecular geometry and local aromaticity of the benzo[g]pteridine core were described using the local HOMED aromaticity indices. The only substituent, which consistently decreases the aromaticity of all rings was —CF_3 bonded to the N(10) atom possibly because of very inductive electron-withdrawing character of the group. The **iCF** derivative is thus the least stable within the studied group. Generally, the smallest changes of the HOMED index were found in the benzene-like A ring mostly due to dimethyl substitution on this ring (0.01). HOMED changes of the heterocyclic B and C rings were larger by one to two tenths depending on the position of the substituent. The substitution using methyl, butyl, phenyl, and 2,3,4,5-tetrahydroxypentyl had minimal effect on the energies of frontier molecular orbitals. Due to the heterocyclic ring substitution, the HOMO–LUMO band gaps were lowered for all cases except for **CF**. TD-B3LYP calculations of optical transitions predicted that the large number of studied derivatives can absorb and emit light in the visible spectral region. Obtained theoretical results can be helpful in the preparation of materials applicable in optoelectronics or medicine in the future.

Acknowledgement

The work has been supported by the Slovak Research and Development Agency (APVV-15-0053) and VEGA 1/0504/20. We are grateful to the HPC center at the Slovak University of Technology in Bratislava, which is a part of the Slovak Infrastructure of High Performance Computing (SIVVP project, ITMS code 26230120002, funded by the European region development funds, ERDF) for the computational time and resources made available.

D.C. would like to thank for the financial support from the STU Grant scheme for Support of Young Researchers (1848).

J.T. thanks the internal grant FCH-S-20-6340 of the Brno University of Technology.

References

Ai Y, Zhang F, Chen S, Luo Y, Fang W (2010) J. Phys. Chem. Lett. 1: 743—747.

Allen FH, Kennard O, Watson DG, Brammer L, Orpen AG, Taylor R (1987) J. Chem. Soc. Perkin Trans. 2.: S1—S19.

Becke AD (1988) Phys. Rev. A 38: 3098—3100.

Cyrañski MK, Krygowski TM, Katritzky AR, Schleyer PvR (2002) J. Org. Chem. 67: 1333—1338.

Flukiger P, Luthi HP, Sortmann S, Weber J (2002) Molekel 4.3, Swiss National Supercomputing Centre, Manno, Switzerland.

Frisch MJ, Trucks GW, Schlegel HB, Scuseria GE, Robb MA, Cheeseman JR, Scalmani G, Barone V, Menucci B, Petersson GA, Nakatsuji H, Caricato M, Li X, Hratchian HP, Izmaylov AF, Bloino J, Zheng G, Sonnenberg JL, Hada M, Ehara M, Toyota K, Fukuda R, Hasegawa J, Ishida M, Nakajima T, Honda Y, Kitao O, Nakai H, Vreven T, Montgomerry JA Jr., Peralta JE, Ogliaro F, Bearpark MJ, Heyd JJ, Brothers EN, Kudin KN, Staroverov VN, Keith TA, Kobayashi R, Normand J, Raghavachari K, Rendell AP, Burant JC, Iyengar SS, Tomasi J, Cossi M, Rega N, Millam JM, Klene M, Knox JE, Cross JB, Bakken V, Adamo C, Jaramillo J, Gomperts R, Stratmann RE, Yazyev O, Austin AJ, Cammi R, Pomelli C, Ochterski JW, Martin RL, Morokuma K, Zakrzewski VG, Voth GA, Salvador P, Dannenberg JJ, Dapprich S, Daniels AD, Farkas O, Foresman JB, Ortiz JV, Cioslowski J, Fox DJ (2013) Gaussian 09, Revision D.01, Gaussian, Inc., Wallingford CT.

Frizzo CP, Martins MAP (2012) Struct Chem 23: 375—380.

Furche F, Ahlrichs R (2002) J. Chem. Phys. 117: 7433.

Grimme S, Waletzke M (1999) J. Chem. Phys. 111(13): 5645—5655.

Gross E, Dobson J, Petersilka M (1996) Top. Curr. Chem. 181: 81.

Hanwell MD, Curtis DE, Lonie DC, Vandermeersch T, Zurek E, Hutchison GR (2012) J. Cheminformatics 4: 17.

Hariharan PC, Pople JA (1973) Theor. Chim. Acta 28: 213—222.

Kozioł J (1966) Photochem. Photobiol. 5: 41.

Lee C, Yang W, Parr RG (1988) Phys. Rev. B 37: 785—789.

Min DB, Boff JM (2006) Comp Rev Food Sci Food Saf. 1(2): 58—72.
Ośmiałowski B, Raczyńska ED, Krygowski TM (2006) J Org Chem 71(10): 3727—3736.
Penzkofer A (2016) J. Photochem. Photobiol. A 314: 114—124.
Rassolov V, Pople JA, Ratner M, Windus TL (1998) J. Chem. Phys. 109: 1223—1229.
Salzmann S, Marian CM (2009) Photochem. Photobiol. Sci. 8: 1655—1666.
Sikorska E, Khmelinskii IV, Bourdelande JL, Bednarek A, Williams SL, Patel M, Worrall DR, Koput J, Sikorski M (2004d) Chem Phys. 301(1): 95—103.
Sikorska E, Khmelinskii IV, Komasa A, Koput J, Ferreira LFV, Herance JR, Bourdelande JL, Williams SL, Worrall DR, Insińska-Rakc M, Sikorski M (2005) Chemical Physics 314: 239—247.
Sikorska E, Khmelinskii IV, Koput J, Sikorski M (2004c) J. Mol. Struct. (Theochem) 676: 155.
Sikorska E, Khmelinskii IV, Prukala W, Williams SL, Patel M, Worrall DR, Bourdelande JL, Koput J, Sikorski M (2004b) J. Phys. Chem. A 108: 1501.
Sikorska E, Khmelinskii IV, Worrall DR, Koput J, Sikorski M (2004a) J Fluoresc. 14(1): 57—64.
Sikorski M, Sikorska E, Worrall DR, Wilkinson D (1998) J. Chem. Soc. 94, 2347—2353.
Zanetti-Polzi L, Aschi M, Daidone I, Amadei A (2017) Chem. Phys. Lett. 669: 119—124.